Stochastic Risk-Constrained Scheduling of Renewable-Powered Autonomous Microgrids with Demand Response Actions: Reliability and Economic Implications

Vahedipour-Dahraie, Mostafa; Rashidizadeh-Kermani, Homa ; Anvari-Moghaddam, Amjad; Guerrero, Josep M.

Published in:
I E E E Transactions on Industry Applications

DOI (link to publication from Publisher):
10.1109/TIA.2019.2959549

Publication date:
2020

Document Version
Accepted author manuscript, peer reviewed version

Stochastic Risk-Constrained Scheduling of Renewable-Powered Autonomous Microgrids with Demand Response Actions: Reliability and Economic Implications

Mostafa Vahedipour-Dahraie, Homa Rashidizadeh-Kermani, Amjad Anvari-Moghaddam, *Senior Member, IEEE*, Josep M. Guerrero, *Fellow, IEEE*

***Abstract*-- The unpredictable and volatile nature of renewable energy sources (RESs) will increase the burden of a system operator for maintaining the system reliability in different conditions. In this paper, a stochastic risk-constrained framework is proposed for short-term optimal scheduling of autonomous microgrids to evaluate the influence of demand response (DR) programs on reliability and economic issues, simultaneously. The objective is to maximize the expected profit of the microgrid operator through optimal scheduling of resources in a more reliable manner considering both supply and demand side uncertainties. In the proposed approach, the microgrid operator's risk aversion is modeled by using the conditional value-at-risk (CVaR) method to control and avoid non-desirable profit distributions due to various system uncertainties. Moreover, AC optimal power flow (AC-OPF) technique is employed to calculate the amount of energy and reserve of dispatchable distributed generation (DG) units and responsive loads for the operational hour of the next day. Eventually, the applicability of the proposed method is studied on different test systems and impacts of various parameters such as level of DR participants and values of lost load (VOLL) as well as risk aversion parameter on the system's economy and reliability indices are investigated deeply.**

***Index Terms*— Demand response, renewable energy sources (RESs), reliability, stochastic scheduling, values of lost load (VOLL).**

NOMENCLATURE

Abbreviations

AC-OPF	AC optimal power flow
CVaR	Conditional value-at-risk
DG	Distributed generation
DR	Demand response
EENS	Expected energy not supplied
ENS	Energy not supplied
EP	Expected profit
LRC	Load rebound characteristic
MCS	Monte-Carlo simulation
PDF	Probability density function
RES	Renewable energy source
RTP	Real-time pricing
VOLL	Values of lost load

Indices and Sets

i, N_{DG}	Index and number of distributed generation (DG) units.
w, N_W	Index and number of wind turbines.
v, N_V	Index and number of photovoltaic (PV) units.
j, N_J	Index and number for group of customers.
s, N_S	Index and number of scenarios.
t, h, N_T	Indices and number of timeslots in the scheduling horizon.
Δt	Duration of interval t
b, n, r	Indices for system buses.

Symbols

$\overline{(.)}, \underline{(.)}$	Maximum (minimum) values of (.).

Parameters and Constants

$D_{j,t}$ ($D^{\text{int}}_{j,t}$)	Demand of customer j at time t after (before) implementing DR program.
$\text{Pr}^{\text{int}}_{j,t}$ ($\text{Pr}^{\text{int}}_{j,h}$)	Initial values of electricity price offered to customer j at time t (h).
α	Confidence level used to compute the CVaR.
β	Weighting parameter modeling the tradeoff between expected profit and CVaR.
M_1, M_2	Large positive scalars.
$S, (S')$	Branch-bus incidence matrix (S' is transpose of matrix S).
a_i, b_i, c_i	Coefficients of operation cost of DG unit i.
UR_i, DR_i	Ramping-down and ramping-up rates of DG unit i.
UT_i, DT_i	Minimum up and down time of DG unit i.
$\text{Pr}_{w,t}$, $\text{Pr}_{v,t}$	Price of energy offered by wind and solar power producers in time period t.
$\text{Pr}_{j,t,s}$	Price of selling electricity to customer j in time t and scenario s.
$\text{Pr}^{R^{up}}_{i,t}$ ($\text{Pr}^{R^{dn}}_{i,t}$)	Bid of up (down)-spinning reserve submitted by DG i in time t.
$\text{Pr}^{R^{up}}_{j,t}$ ($\text{Pr}^{R^{dn}}_{j,t}$)	Bid of up (down)-spinning reserve submitted by load j in time t.
$\text{Pr}^{R^{non}}_{i,t}$	Bid of non-spinning reserve submitted by unit i in time t.
$E^{j}_{t,t}$	Self-elasticity of period t.

$E_{t,h}^{j}$	Cross elasticity of period *t* to period *h*.
ρ_s	Occurrence probability of scenario *s*.
$G_{n,r}$ ($B_{n,r}$)	The line conductance and susceptance (from bus n to r).
$LOL_{j,t,s}$	Load shedding imposed on customer *j* at time t and scenario s.
$Q_{j,t,s}^{shed}$	Involuntarily reactive power shed by customer *j* at time *t* and scenario *s*.
$\theta_{i,t,s}$, $\theta_{w,t,s}$, $\theta_{j,t,s}$	Power factor of DG *i*, wind turbine *w*, and load *j* at time *t* and scenario *s*.
M	Mapping of the set of generating units (loads) into the set of nodes.
Λ	Set of lines.

Variables

$D_{j,t,s}$ ($Q_{j,t,s}$)	Active (reactive) power consumed by customer *j* in period *t* and scenario *s*.
D	Total demand vector.
$LF_{n,r}^{P}$ ($LF_{n,r}^{Q}$)	Active (reactive) power flow from node *n* to *r*.
LF	Power flow limit vector.
$P_{i,t,s}$ ($Q_{i,t,s}$)	Scheduled active (reactive) power for DG unit *i* at time *t* and scenario *s*.
$P_{w,t,s}$ ($Q_{w,t,s}$)	Output active (reactive) power of wind turbine *w* at time *t* and scenario *s*.
$P_{v,t,s}$ ($Q_{v,t,s}$)	Output active (reactive) power of PV *v* at time *t* and scenario *s*.
$R_{j,t}^{up}$ ($R_{j,t}^{dn}$)	Up- (down-) spinning reserves scheduled by load *j* at time *t*.
$R_{i,t}^{up}$ ($R_{i,t}^{dn}$)	Up- (down-) spinning reserves scheduled by DG unit *i* at time *t*.
$R_{i,t}^{non}$	Non-spinning reserve scheduled by DG unit *i* at time *t*.
$r_{i,t,s}^{dn}$ ($r_{j,t,s}^{dn}$)	Down-spinning reserve deployed by unit *i* (load *j*) at time *t* and scenario *s*.
$r_{i,t,s}^{up}$ ($r_{j,t,s}^{up}$)	Up-spinning reserve deployed by unit *i* (load *j*) at time *t* and scenario *s*.
$r_{i,t,s}^{non}$	Non-spinning reserve deployed by DG *i* at time *t* and scenario *s*.
$V_{n,t,s}$ ($\delta_{n,t,s}$)	Voltage magnitude (voltage angle) at node *n* at time *t* and scenario *s*.
ξ	Value-at-risk.
η_s	Auxiliary variable for computing CVaR.
$u_{i,t,s}$	Binary variable denoting commitment status of DG unit *i* at time *t* and scenario *s*.
$y_{i,t,s}$, $z_{i,t,s}$	Binary variables denoting start-up/shut-down of DG unit *i* at time *t* and scenario *s*.

I. Introduction

Microgrids as key players in smart grids, comprised of distributed energy resources (including dispatchable distributed generation (DG) units and renewable energy sources (RESs)), energy storage systems and controllable loads, can operate in both grid-connected and islanded modes [1]. The uncertainty related to RESs and loads can pose a serious challenge to microgrid reliability [2], and negatively affect the ability of a microgrid to provide power to the customers at required power quality [3]. In such condition, demand response (DR) programs can play a significant role to manage the demand load and enhance the reliability of microgrid [4]. Developing smart equipment in modern power systems brings the capability to facilitate the active participation of responsive loads in DR programs [5]. In a system that integrates renewable generation at high rates, DR can also be a useful option to cope with the uncertainty of RESs production [6]-[7].

Evaluation of system reliability when DR programs are implemented has been reported in some research works over the past years [8]-[18]. In [8] a security-constrained model has been proposed to coordinate supply and demand sides toward making a flexible, secure and economic grid. In the proposed method, generation units are committed to enhance the flexibility by providing up- and down-spinning reserves while an optimal real-time pricing (RTP) scheme provides demand-side flexibility. In [9], impact of DR programs on short-term reliability assessment of wind integrated power systems has been addressed by using Monte-Carlo simulation (MCS). Although authors in [8]-[9] have discussed the reliability benefits made by implementing DR programs, they have not discussed the reliability implications of DR to increase the utilization of the existing network and the DR benefits associated with this objective. Authors in [10] have proposed an optimization-based method to incorporate the customer satisfaction in the energy management programs. The impact of different DR programs has been studied on reliability of distribution systems considering different participation levels of customers in energy management programs. In [11], an optimization framework has been presented when emergency DR and emergency loading of overhead lines are integrated within the network operator's flexibility strategy. The proposed optimization enables the operator to make a tradeoff between ageing and reliability costs and DR costs. In [12], a reliability-constrained decision-making model for energy service provider has been presented incorporating DR programs. In the same work, the compensation cost of energy not supplied (ENS) has been considered by formulating reliability constraints. Also, the potential of DR actions for reducing total cost and improving technical aspects has been investigated in a distribution network. In [13], a reliability evaluation method of smart distribution systems has been proposed, in which the load rebound characteristics (LRC) is considered and the expected ENS (EENS) is modified accordingly. The status of controlled load during an outage and after repairing the outage has been described in that work, and the effects of LRC on reliability indices of distribution systems have been quantitatively revealed.

In a few of the reviewed literatures, the researchers present stochastic scheduling models to effectively manage the demand-side participation in order to enhance the system reliability under uncertainties. In optimization problems under uncertainty where a stochastic programming model is developed, the risk management plays an important role in providing valuable information to decision makers. In [14] an optimal management system for battery energy storage has

been proposed in a way to enhance the resilience of a microgrid while maintaining its operational cost at a minimum level. The optimization goal is achieved by solving a linear programming problem while the conditional value-at-risk (CVaR) is incorporated in the objective function. Moreover, in [15] power scheduling and bidding problem for a microgrid aggregator has been formulated as a scenario-based stochastic program, in which risk control has been embedded in the problem by employing CVaR approach. Although, the impacts of risk measurement on different decision-making problems have been addressed by several researchers, only few research works have investigated the impact of risk aversion of the operator on the microgrid reliability. In [16] a risk-constrained stochastic framework has been presented for jointly energy and reserve scheduling considering CVaR concept. Nevertheless, in none of the mentioned works, the effects of reliability indices on the microgrid scheduling have been investigated. Instead, a risk-constrained stochastic model has been proposed in [17] for joint energy and reserve scheduling to maximize the expected profit of an islanded microgrid operator where the risk averse behavior of the operator is modeled by implementing CVaR method. Likewise, authors in [18] have proposed a two-stage stochastic model for optimal security constrained energy and reserve scheduling in an autonomous microgrid with price-responsive loads. In the same work, an economic-based DR model based on consumers' preferences has been developed and the effect of RTP-based DR programs on frequency security of an islanded microgrid has been investigated.

This paper extends our previous work presented in [18] by developing a stochastic scheduling framework and investigating the impact of value of lost load (VOLL) on an autonomous microgrid reliability and economy, simultaneously. The scope of models in technical literature and the scope and contribution of this paper is summarized in Table I. Compared to the existing studies in this area, there are main differences between this work and the others. First, the economy and reliability performance of the autonomous microgrids is assessed in different levels of DR participants by using a proper stochastic model, in which AC-optimal power flow (AC-OPF) is used in each working condition to ensure the validity of solution in terms of voltage and frequency security. It should be noted that, most of the recent works use DC-power flow (DC-OPF) methodologies in connection with their optimization problems which in turn neglect reactive power flows and their impact on the system reliability indices. Second, in the proposed approach, the microgrid operator's risk aversion is modeled by using the CVaR method to control and avoid non-desirable profit distributions due to various system uncertainties. This enables the microgrid operator to select a desirable risk level prior to solving the stochastic optimization model and making final decisions from both of economy and reliability viewpoints. In addition, in this study the sensitivity of the expected profit and the CVaR respect to reliability indices and level of DR participants are investigated.

As a whole, the novelty aspects of this study, compared to the existing literature in this subject area, are summarized as follows:

1) A risk-constrained stochastic framework is presented for joint energy and reserve scheduling of autonomous microgrids by considering reliability issues as well as all the pertinent uncertainties associated with loads, RESs available power and electricity prices.
2) The risk associated with profit variability is explicitly taken into account in the problem formulation through the incorporation of CVaR metric. This enables the microgrid operator to select a desirable risk level prior to solving the stochastic optimization model and making final decisions.
3) Impacts of various parameters such as level of DR participants, VOLL index and risk aversion parameter on the reserve capacity allocation, economy and reliability indices are explored via sensitivity analyses. Moreover, economic benefits and reliability indices in two cases of risk-neutral and risk-averse are compared.

The remaining part of the paper is organized as follows. Section II presents the optimization problem and modeling approach in an uncertain environment. Section III describes stochastic optimization approach. Section IV presents case studies together with simulation results. Finally, conclusions are drawn in sections V.

II. Problem Description and Modeling Approach

A. Problem Description

The paper addresses the short-term scheduling of an autonomous microgrid for maximizing the expected profit of

TABLE I
SUMMARY OF LITERATURE REVIEW AND SCOPE AND CONTRIBUTION OF THIS STUDY

Reference	Stochastic	Risk Measure	Reliability issue	Frequency security	Voltage security	Reserve scheduling	RESs uncertainty	DR uncertainty	Power flow
[6], [7]	✓			✓			✓		DCOPF
[8], [9]	✓		✓	✓				✓	DCOPF
[10], [11], [12], [13]	✓		✓	✓			✓	✓	DCOPF
[14], [15]	✓	✓					✓	✓	DCOPF
[16]	✓	✓				✓	✓	✓	DCOPF
[17]	✓	✓	✓			✓	✓	✓	DCOPF
[18]	✓	✓		✓	✓	✓	✓	✓	ACOPF
Proposed Model	✓	✓	✓	✓	✓	✓	✓	✓	ACOPF

the operator by considering reliability aspects. It is supposed that the operator interacts with take-or-pay contract [19] to purchase energy from dispatchable DGs and wind generation units while it sells electricity to customers under day-ahead/real-time prices, which is based on a service agreement. In addition, the operator has accessibility to the historical data including demand load, wind power forecasts, and electricity prices for the scheduling horizon. Customers have two load categories; i.e., responsive loads and fixed loads. They are also assumed to be equipped with smart metering and advanced energy management systems which enable them to respond to dynamic tariffs. Based on operating conditions of the system, responsive loads can adjust their demand by shedding or/and shifting option to reduce the electricity bills. In contrast, there is no control over fixed loads and they should be supplied at all circumstances. Additionally, the customers can participate in providing up- (down-) spinning reserve capacities and deploy them when frequency regulation is needed (e.g., during low (high) wind periods). Therefore, both DG units and responsive loads can activate a portion of their scheduled reserve capacity to compensate deviations between the scheduled powers in day-ahead and actual ones in real-time. Additionally, in this paper, CVaR criterion is implemented to manage the risks that operator may experience during undesired scenarios in the microgrid operation process. The proposed problem is formulated as a mixed-integer linear programming (MILP) model that can be solved by off-the-shelf packages, such as CPLEX and GUROBI.

B. Modeling the Demand Response Programs

In this study, RTP-based DR program is used to encourage the consumers to change their electricity consumption pattern (considering load shifting and curtailment options) in response to fluctuations of price over the time [20], [21]. The influence of RTP-based DR program on customers' power consumption can be described by the concept of elasticity of demand. Elasticity, that is defined as the sensitivity of the demand with respect to the price, is used to estimate the load reduction and load recovery by DR participants. Therefore, the price elasticity of customer *j* in time slot *t* versus time slot *h* can be defined as [22], [23]:

$$E_{t,h}^{j}=\frac{\mathrm{Pr}_{j,h}^{\mathrm{int}}}{D_{j,t}^{\mathrm{int}}}\cdot\frac{\partial D_{j,t}}{\partial \mathrm{Pr}_{j,h}} \tag{1}$$

when $h = t$, (1) represents self-elasticity of a customer and its attitude toward load curtailment. Otherwise, (1) represents cross-elasticity and considers the shift of demand to another time period due to a change in price at the current period. By participating in DR programs, in order to achieve the maximum benefit, customer *j* changes its demand in period *t* from $D_{j,t}^{\mathrm{int}}$ to $D_{j,t}$ as:

$$D_{j,t}=D_{j,t}^{\mathrm{int}}+\Delta D_{j,t} \tag{2}$$

The amount of customer's profit, $S(D_{j,t})$, is obtained from the benefits, $B(D_{j,t})$, minus the energy costs as (3), [18].

$$S(D_{j,t})=B(D_{j,t})-D_{j,t}\,\mathrm{Pr}_{j,t} \tag{3}$$

In order to maximize the profit of customer *j*, (4) must be met.

$$\frac{\partial S(D_{j,t})}{\partial D_{j,t}}=0\Rightarrow\frac{\partial B(D_{j,t})}{\partial D_{j,t}}=\mathrm{Pr}_{j,t} \tag{4}$$

Here, a quadratic utility function is used to incentivize the participation of responsive loads in DR programs. Based on the model, the utility of customer's *j* is obtained as:

$$B(D_{j,t})=B_{j,t}^{\mathrm{int}}+\sum_{h=1}^{N_T}[\frac{\mathrm{Pr}_{j,h}^{\mathrm{int}}D_{j,t}}{1+(E_{t,h}^{j})^{-1}}\times(\frac{D_{j,t}}{D_{j,t}^{\mathrm{int}}})^{(E_{t,h}^{j})^{-1}}-1] \tag{5}$$

Differentiating (5) with respect to $D_{j,t}$ gives:

$$\begin{aligned}\frac{\partial B(D_{j,t})}{\partial D_{j,t}}=&\sum_{h=1}^{N_T}\frac{\mathrm{Pr}_{j,h}^{\mathrm{int}}}{1+(E_{t,h}^{j})^{-1}}\times[(\frac{D_{j,t}}{D_{j,t}^{\mathrm{int}}})^{(E_{t,h}^{j})^{-1}}-1]\\&+\sum_{h=1}^{N_T}\frac{\mathrm{Pr}_{j,h}^{\mathrm{int}}D_{j,t}}{1+(E_{t,t}^{j})^{-1}}\times[(E_{t,h}^{j})^{-1}\frac{1}{D_{j,t}^{\mathrm{int}}}(\frac{D_{j,t}}{D_{j,t}^{\mathrm{int}}})^{(E_{t,h}^{j})^{-1}-1}]\end{aligned} \tag{6}$$

Substituting (6) into (4) yields:

$$\begin{aligned}&\sum_{h=1}^{N_T}[1+(E_{t,h}^{j})^{-1}]\times\sum_{h=1}^{N_T}\frac{\mathrm{Pr}_{j,h}}{\mathrm{Pr}_{j,h}^{\mathrm{int}}}=\\&\quad 1-\sum_{h=1}^{N_T}[1+(E_{t,h}^{j})^{-1}]\times(\frac{D_{j,t}}{D_{j,t}^{\mathrm{int}}})^{(E_{t,h}^{j})^{-1}}\end{aligned} \tag{7}$$

By some simplifications the following equation is achieved:

$$(\frac{D_{j,t}}{D_{j,t}^{\mathrm{int}}})^{(E_{t,h}^{j})^{-1}}-\sum_{h=1}^{N_T}\frac{1}{1+(E_{t,h}^{j})^{-1}}=\sum_{h=1}^{N_T}\frac{\mathrm{Pr}_{j,h}}{\mathrm{Pr}_{j,h}^{\mathrm{int}}} \tag{8}$$

Equation (8) should be re-written as follows:

$$(\frac{D_{j,t}}{D_{j,t}^{\mathrm{int}}})^{(E_{t,h}^{j})^{-1}}=\sum_{h=1}^{N_T}[(\frac{\mathrm{Pr}_{j,h}}{\mathrm{Pr}_{j,h}^{\mathrm{int}}}+\frac{1}{1+(E_{t,h}^{j})^{-1}})] \tag{9}$$

$$D_{j,t}=D_{j,t}^{\mathrm{int}}\sum_{h=1}^{N_T}[(\frac{\mathrm{Pr}_{j,h}}{\mathrm{Pr}_{j,h}^{\mathrm{int}}}+\frac{1}{1+(E_{t,h}^{j})^{-1}})^{E_{t,h}^{j}}] \tag{10}$$

$$D_{j,t}=D_{j,t}^{\mathrm{int}}\prod_{h=1}^{N_T}[(\frac{\mathrm{Pr}_{j,h}}{\mathrm{Pr}_{j,h}^{\mathrm{int}}}+\frac{1}{1+(E_{t,h}^{j})^{-1}})^{E_{t,h}^{j}}] \tag{11}$$

Equation (11) denotes the optimal amount of demand from customers' point of view by participating in price-based DR programs.

C. Reliability Evaluation Procedure

The conventional reliability indices such as EENS are usually used to assess long-term security of energy supply [24]. This index has been redefined here to evaluate the reliability of energy provision in a given period. Therefore, the *EENS (T)* is defined as the expected *ENS* during the operational horizon *T* and can be calculated as follows [24]:

$$EENS=\sum_{t=1}^{N_T}\sum_{s=1}^{N_S}\sum_{j=1}^{N_J}\rho_s LOL_{j,t,s}\Delta t \tag{12}$$

where, ρ_s is the probability of occurrence of scenario *s*, Δt is the duration of time period *t* which can be five minutes or more and $LOL_{j,t,s}$ is the loss of load (LOL) of consumer *j* in period *t* during operating scenario *s*.

D. Objective Function

The objective function (OF) of the problem is to maximize the expected profit (*EP*) of the operator considering risk constraints, DR and reliability issues. Detailed mathematical optimization for the operator over all the possible realization scenarios of load, electricity price and RESs power is formulated as follows:

$$OF: Max(EP) = Income - \mathrm{Cost}_E - \mathrm{Cost}_R + \beta CVaR \tag{13}$$

where, *Income* is total income of microgrid operator, and $Cost_E$ and $Cost_R$ are total operation cost (or cost of energy provision) and the cost of scheduled reserve capacity, respectively. The cost of energy includes the operation cost of dispatchable DG units ($\mathrm{Cost_{DGs}}$), cost of RESs ($\mathrm{Cost_{RESs}}$), cost of customers' participation in DR ($\mathrm{Cost_{DR}}$), and cost of ENS ($\mathrm{Cost_{ENS}}$). Also, the cost of reserve capacity includes cost of reserves allocated by DG units and DR. Different terms in (14) are formulated in the following.

Income includes the revenue from selling energy to customers which is formulated as follows:

$$Income = \sum_{t=1}^{N_T}\sum_{s=1}^{N_S}\sum_{j=1}^{N_J} \rho_s \,\mathrm{Pr}_{j,t,s}\, D_{j,t,s}\Delta t \tag{14}$$

where, $\mathrm{Pr}_{j,t,s}\, D_{j,t,s}$ shows the operator's revenue by selling electricity to the customer *j* at time *t* for scenario *s*. Moreover, $Cost_E$ can be formulated as:

$$Cost_E = Cost_{DGs} + Cost_{RESs} + Cost_{DR} + Cost_{ENS} \tag{15}$$

Term of $\mathrm{Cost_{DGs}}$ consists of generation cost, start-up cost and shut-down cost that is represented as follows:

$$Cost_{DGs} = \sum_{t=1}^{N_T}\sum_{s=1}^{N_S}\rho_s \sum_{i=1}^{N_{DG}} \begin{bmatrix} a_i + b_i P_{i,t,s} + c_i P_{i,t,s}^2 + \\ SU_{i,t,s} + SD_{i,t,s} \end{bmatrix} \Delta t \tag{16}$$

The term $\mathrm{Cost_{RESs}}$ stands for the cost of power provision from RES units. In this paper, wind and photovoltaic (PV) units are considered as privately owned renewable resources, thus, the operator has to pay for their commitments. Therefore, $\mathrm{Cost_{RESs}}$ represents as follows:

$$\mathrm{Cost}_{RESs} = \sum_{t=1}^{N_T}\sum_{s=1}^{N_S}\rho_s \begin{pmatrix} \sum_{w=1}^{N_W} \mathrm{Pr}_{w,t}\, P_{w,t,s} + \\ \sum_{v=1}^{N_V} \mathrm{Pr}_{v,t}\, P_{v,t,s} \end{pmatrix} \Delta t \tag{17}$$

In the price-based DR program, the operator pays the customers based on hourly electricity price ($\mathrm{Pr}_{j,t,s}$). This cost can be formulated as follows:

$$Cost_{DR} = \sum_{t=1}^{N_T}\sum_{s=1}^{N_S}\rho_s \sum_{j=1}^{N_J} \Delta D_{j,t,s}\, \mathrm{Pr}_{j,t,s}\, \Delta t \tag{18}$$

where, $\Delta D_{j,t,s}$ denotes the amount of demand of customer *j* at time *t* and scenario *s*. Therefore, $\Delta D_{j,t,s}\,\mathrm{Pr}_{j,t,s}$ represents the payments to customer *j* for his DR participants.

Finally, $\mathrm{Cost_{ENS}}$ denotes the *LOL* cost that should be considered as reliability improvement measure.

$$\mathrm{Cost}_{ENS} = \sum_{t=1}^{N_T}\sum_{s=1}^{N_S}\sum_{j=1}^{N_J} \rho_s (VOLL \times LOL_{j,t,s})\Delta t \tag{19}$$

Moreover, the cost of reserve capacity for microgrid, which is allocated to dispatchable DG units and DR, can be formulated as follows [25]:

$$Cost_R = \sum_{t=1}^{N_T} \begin{pmatrix} \sum_{j=1}^{N_{DG}} (\mathrm{Pr}_{i,t}^{R^{up}}\, R_{i,t}^{up} + \mathrm{Pr}_{i,t}^{R^{dn}}\, R_{i,t}^{dn} + \\ \mathrm{Pr}_{i,t}^{R^{non}}\, R_{i,t}^{non}) + \\ \sum_{j=1}^{N_J} (\mathrm{Pr}_{j,t}^{R^{up}}\, R_{j,t}^{up} + \mathrm{Pr}_{j,t}^{R^{dn}}\, R_{j,t}^{dn}) \end{pmatrix} \tag{20}$$

In (20), the first and the second lines represent the cost of scheduled up/down- and non- spinning reserves of DG units, respectively. The third line denotes the cost of scheduled up/down spinning reserves of responsive loads. Furthermore, last term of the objective function is CVaR that is multiplied by a risk factor. In the proposed model, CVaR method is used to model the trade-off between maximizing expected profit of the operator and the risk of obtaining low profits in undesired scenarios. CVaR for a confidence level α is given as follow [17]:

$$CVaR = \max_{\xi,\eta_s}[\xi - (1-\alpha)^{-1}\sum_{s=1}^{N_S}\rho_s\eta_s] \tag{21}$$

Subject to:

$$\eta_s + B_s - \xi \geq 0; \quad \eta_s \geq 0 \tag{22}$$

where, parameter α represents the confidence level of risk and is usually assigned a value within the range of 0.90–0.99. Also, B_s is the profit in scenario *s* and ξ represents the greatest value of the profit such that the probability of experiencing a profit less than or equal to ξ is less than or equal to 1-α. At the optimum, the auxiliary variable η_s represents the excess of ξ over the profit of scenario *s*, provided that this excess is positive [17].

E. Constraints of the Problem

The proposed objective function is satisfied with the following constraints:

Demand-supply power balance in each time and working condition must be met as follows:

$$\begin{aligned} &\sum_{i:(i,n)\in M_I(t,s)} P_{i,t,s} + \sum_{w:(w,n)\in M_W(t,s)} P_{w,t,s} + \sum_{v:(v,n)\in M_V(t,s)} P_{v,t,s} \\ &\quad - \sum_{j:(j,n)\in M_L(t,s)} (D_{j,t,s} - LOL_{j,t,s}) = \sum_{r:(n,r)\in\Lambda(t,s)} LF_{n,r,t,s}^{P} \end{aligned} \tag{23}$$

$$\begin{aligned} &\sum_{i:(i,n)\in M_I(t,s)} Q_{i,t,s} + \sum_{w:(w,n)\in M_W(t,s)} Q_{w,t,s} + \sum_{v:(v,n)\in M_V(t,s)} Q_{v,t,s} \\ &\quad - \sum_{j:(j,n)\in M_J(t,s)} (Q_{j,t,s} - Q_{j,t,s}^{shed}) = \sum_{r:(n,r)\in\Lambda(t,s)} LF_{n,r,t,s}^{Q} \end{aligned} \tag{24}$$

where, $LF_{n,r,t,s}^{P}$ and $LF_{n,r,t,s}^{Q}$ represent the active and reactive power flows from bus *n* to bus *r* calculated as follow:

$$LF_{n,r,t,s}^{P} = \begin{bmatrix} G_{n,r}\left[V_{n,t,s}^2 - V_{n,t,s}V_{r,t,s}\cos(\delta_{n,t,s} - \delta_{r,t,s})\right] \\ -B_{n,r}V_{n,t,s}V_{r,t,s}\sin(\delta_{n,t,s} - \delta_{r,t,s}) \end{bmatrix} \tag{25}$$

$$LF^{Q}_{n,r,t,s} = -\begin{bmatrix} B_{n,r}\left[V^{2}_{n,t,s} - V_{n,t,s}V_{r,t,s}\cos(\delta_{n,t,s} - \delta_{r,t,s})\right] \\ + G_{n,r}V_{n,t,s}V_{r,t,s}\sin(\delta_{n,t,s} - \delta_{r,t,s}) \end{bmatrix} \quad (26)$$

When the microgrid faces a capacity shortage in a working scenario, the mandatory load shedding can be employed to maintain system security. Due to high cost of lost load, the amount of $LOL_{j,t,s}$ should not exceed a limit as follow [17]:

$$0 \le LOL_{j,t,s} \le \overline{LOL}_{j,t} \quad (27)$$

By assuming power factor $\theta_{j,t}$ for consumer *j*, its involuntarily reactive power curtailment at time t and scenario s ($Q^{shed}_{j,t,s}$) is calculated as follow:

$$Q^{shed}_{j,t,s} = LOL_{j,t,s}\cos(\tan^{-1}(\theta_{j,t})) \quad (28)$$

Other operating constraints that model the real-time operation of microgrid include voltage magnitude limit (29), voltage angle limit (30), line flow limits (31), production limits of units (32) and reactive power limits of DGs and RESs (33)-(35), which are presented as follows:

$$\underline{V}_n \le V_{n,t,s} \le \overline{V}_n \quad (29)$$

$$-\pi \le \delta_{n,t,s} \le \pi \quad (30)$$

$$(LF^{P}_{n,r,t,s})^2 + (LF^{Q}_{n,r,t,s})^2 \le (\overline{LF}_{n,r})^2 \quad (31)$$

$$\underline{P}_k \le P_{k,t,s} \le \overline{P}_k \qquad k \in \{i, w, v\} \quad (32)$$

$$Q_{i,t,s} = P_{i,t,s}\cos(\tan^{-1}(\theta_{i,t,s})) \quad (33)$$

$$Q_{w,t,s} = P_{w,t,s}\cos(\tan^{-1}(\theta_{w,t,s})) \quad (34)$$

$$Q_{v,t,s} = 0 \quad (35)$$

Constraints (36) and (37) represent the increment or decrement limit of produced power by DG units in a specified period in each scenario, respectively.

$$P_{i,t,s} - P_{i,t-1,s} \le UR_i(1 - y_{i,t,s}) + \underline{P}_i\, y_{i,t,s} \quad (36)$$

$$P_{i,t-1,s} - P_{i,t,s} \le DR_i(1 - z_{i,t,s}) + \underline{P}_i\, z_{i,t,s} \quad (37)$$

where, UR_i and DR_i are the ramping-down and ramping-up rates limit of DG unit *i*, respectively. The minimal down and up time limitations of DGs are determined by (38) and (39), respectively.

$$\sum_{h=t}^{t+UT_i-1} u_{i,t,s} \ge UT_i\, y_{i,t,s} \quad (38)$$

$$\sum_{h=t}^{t+DT_i-1} (1 - u_{i,t,s}) \ge DT_i\, z_{i,t,s} \quad (39)$$

where, UT_i and DT_i are the minimum up and down time of DG unit *i*, respectively. In addition, the relationship between start-up and shut-down binary variables in a unit commitment problem should be considered as (40) and (41), respectively [15].

$$y_{i,t,s} - z_{i,t,s} = u_{i,t,s} - u_{i,t-1,s} \quad (40)$$

$$y_{i,t,s} + z_{i,t,s} \le 1 \quad (41)$$

The limit of allocated up, down and non-spinning reserves by DG units to fully regulate the system frequency should be defined as:

$$0 \le R^{up}_{i,t} \le \overline{P}_i u_{i,t} - P_{i,t} \quad (42)$$

$$0 \le R^{dn}_{i,t} \le P_{i,t} - \underline{P}_i u_{i,t} \quad (43)$$

$$0 \le R^{non}_{i,t} \le \overline{P}_i\,(1 - u_{i,t}) \quad (44)$$

Moreover, constraints (45) and (46) represent up and down-spinning reserves allocated by responsive loads in each time and scenario.

$$0 \le R^{up}_{j,t} \le D_{j,t} - \underline{D}_{j,t} \quad (45)$$

$$0 \le R^{dn}_{j,t} \le \overline{D}_{j,t} - D_{j,t} \quad (46)$$

Moreover, the constraints (47) and (48) couple the scheduled power with possible realizations of stochastic processes.

$$P_{i,t,s} = P_{i,t} + r^{up}_{i,t,s} + r^{non}_{i,t,s} - r^{dn}_{i,t,s} \quad (47)$$

$$D_{j,t,s} = D_{j,t} - r^{up}_{j,t,s} + r^{dn}_{j,t,s} \quad (48)$$

The relationship between scheduled and deployed reserves are represented by (49)-(53), [17].

$$0 \le r^{up}_{i,t,s} \le R^{up}_{i,t} \quad (49)$$

$$0 \le r^{dn}_{i,t,s} \le R^{dn}_{i,t} \quad (50)$$

$$0 \le r^{non}_{i,t,s} \le R^{non}_{i,t} \quad (51)$$

$$0 \le r^{up}_{j,t,s} \le R^{up}_{j,t} \quad (52)$$

$$0 \le r^{dn}_{j,t,s} \le R^{dn}_{j,t} \quad (53)$$

In order to guarantee a reliable generation scheduling the upper limit of the LOL should not exceed customers' demand at that hour. Therefore, the EENS at time *t* is limited as:

$$0 \le EENS_t \le \overline{EENS}_t \quad (54)$$

F. Linearization Procedure

In order to improve the robustness and the computational efficiency of the proposed solution, nonlinear equations such as AC power flow constraints (i.e. equations (26) and (27)) should be linearized to be appropriate for linear programming model. Considering the typical range of voltage amplitude (i.e., $0.95 \le V_{n,t,s} \le 1.05$), these equations are approximated with (55) and (56) with a negligible error [2].

$$LF^{P}_{n,r,t,s} = G_{n,r}(V_{n,t,s} - V_{n,t,s} - \omega_{n,r,t,s} + 1) - B_{n,r}(\delta_{n,t,s} - \delta_{r,t,s}) \quad (55)$$

$$LF^{Q}_{n,r,t,s} = -B_{n,r}(V_{n,t,s} - V_{n,t,s} + \omega_{n,r,t,s} + 1) - G_{n,r}(\delta_{n,t,s} - \delta_{r,t,s}) \quad (56)$$

Over a typical range of voltage angle, i.e., $|\delta_{n,t,s} - \delta_{r,t,s}| \le 10^{\circ}$, $\omega_{n,r,t,s}$ represents the piecewise linear approximation of $\cos(\delta_{n,t,s} - \delta_{r,t,s})$ that is [26],

$$\omega_{n,r,t,s} = d_{n,r,t,s,m}(\delta_{n,t,s} - \delta_{r,t,s}) + e_{n,r,t,s,m} \quad (57)$$

where, $d_{n,r,t,s,m}$ and $e_{n,r,t,s,m}$ are chosen so that $\omega_{n,r,t,s}$ and $\cos(\delta_{n,t,s} - \delta_{r,t,s})$ intersect at break points. The approximation

errors associated with this model can be found in [27]. The active and reactive power flow should be satisfied by (58) and (59), respectively.

$$-\overline{LF}^{P}_{n,r,t,s} \le LF^{P}_{n,r,t,s} \le \overline{LF}^{P}_{n,r,t,s} \quad (58)$$

$$-\overline{LF}^{Q}_{n,r,t,s} \le LF^{Q}_{n,r,t,s} \le \overline{LF}^{Q}_{n,r,t,s} \quad (59)$$

However, to eliminate the non-linear terms $\left(LF^{P}_{n,r,t,s}\right)^2$ and $\left(LF^{Q}_{n,r,t,s}\right)^2$ in equation (31), they are replaced with two new variables defined as $\psi^{P}_{n,r,t,s} \overset{\Delta}{=} \left(LF^{P}_{n,r,t,s}\right)^2$ and $\psi^{Q}_{n,r,t,s} \overset{\Delta}{=} \left(LF^{Q}_{n,r,t,s}\right)^2$. Accordingly, the following constraints are incorporated to relate the new variables to the problem decision variables [2], [28]:

$$0 \le \psi^{P}_{n,r,t,s} \le M_1 LF^{P}_{n,r,t,s}, \quad if: LF^{P}_{n,r,t,s} \ge 0 \quad (60)$$

$$0 \le \psi^{P}_{n,r,t,s} \le -M_1 LF^{P}_{n,r,t,s}, \quad if: LF^{P}_{n,r,t,s} < 0 \quad (61)$$

$$0 \le \psi^{Q}_{n,r,t,s} \le M_2 LF^{Q}_{n,r,t,s}, \quad if: LF^{Q}_{n,r,t,s} \ge 0 \quad (62)$$

$$0 \le \psi^{Q}_{n,r,t,s} \le -M_2 LF^{Q}_{n,r,t,s}, \quad if: LF^{Q}_{n,r,t,s} < 0 \quad (63)$$

$$-M_1 \le \psi^{P}_{n,r,t,s} - LF^{P}_{n,r,t,s} \le M_1 \quad (64)$$

$$-M_2 \le \psi^{Q}_{n,r,t,s} - LF^{Q}_{n,r,t,s} \le M_2 \quad (65)$$

where, M_1 and M_2 are sufficiently large constants. If $LF^{Q}_{n,r,t,s} \ge 0$, according to (60), the limitation of $\psi^{P}_{n,r,t,s}$ can be determined and if $LF^{P}_{n,r,t,s} < 0$, the limitation of $\psi^{P}_{n,r,t,s}$ would be obtained using (61). Similar constraints could be applied to limit the $\psi^{Q}_{n,r,t,s}$ according to changes in $LF^{Q}_{n,r,t,s}$ which are reflected in (62)-(63). In addition, to obtain a feasible region in the linearization process, the values of $\psi^{P}_{n,r,t,s} - LF^{P}_{n,r,t,s}$ and $\psi^{Q}_{n,r,t,s} - LF^{Q}_{n,r,t,s}$ should be limited by (64) and (65), respectively [2].

III. Stochastic Optimization Approach

Fig. 1 illustrates the proposed framework for the stochastic scheduling of the examined microgrid. As can be observed, the input data includes two categories information: probabilistic and deterministic. In day-ahead scheduling process, the microgrid operator faces various uncertainties associated with wind and PV output power, load demand and electricity price. To deal with these uncertainties, the mentioned stochastic variables are characterized by a set of scenarios. To generate scenarios of each stochastic variable, firstly, forecasting errors are calculated for each hour of the next day. Forecasting errors of the stochastic variables are modeled with probability density functions (PDF) for each interval with a zero-mean normal distribution and different standard deviations [15], [29]. In this study, each PDF is divided into seven discrete intervals with different probability levels [17], [30]. MCS is used to generate a large number of scenarios indicating the uncertain parameters based on their hourly PDFs [31]. To solve a stochastic optimization problem, a scenario tree is subsequently built based on the generated scenarios of all stochastic variables [18]. Each scenario captures the information of the hourly wind and PV output power, and the hourly load, in the operating day. To reduce the computational burden of the stochastic procedure, K-means algorithm [32] is applied to mitigate the number of scenarios into a limited set providing well enough the uncertainties.

After scenario generation and reduction, the stochastic scheduling problem is solved for all working scenarios. Using Benders' algorithm, each of these distinct procedures is decomposed into a master problem and a sub-problem.

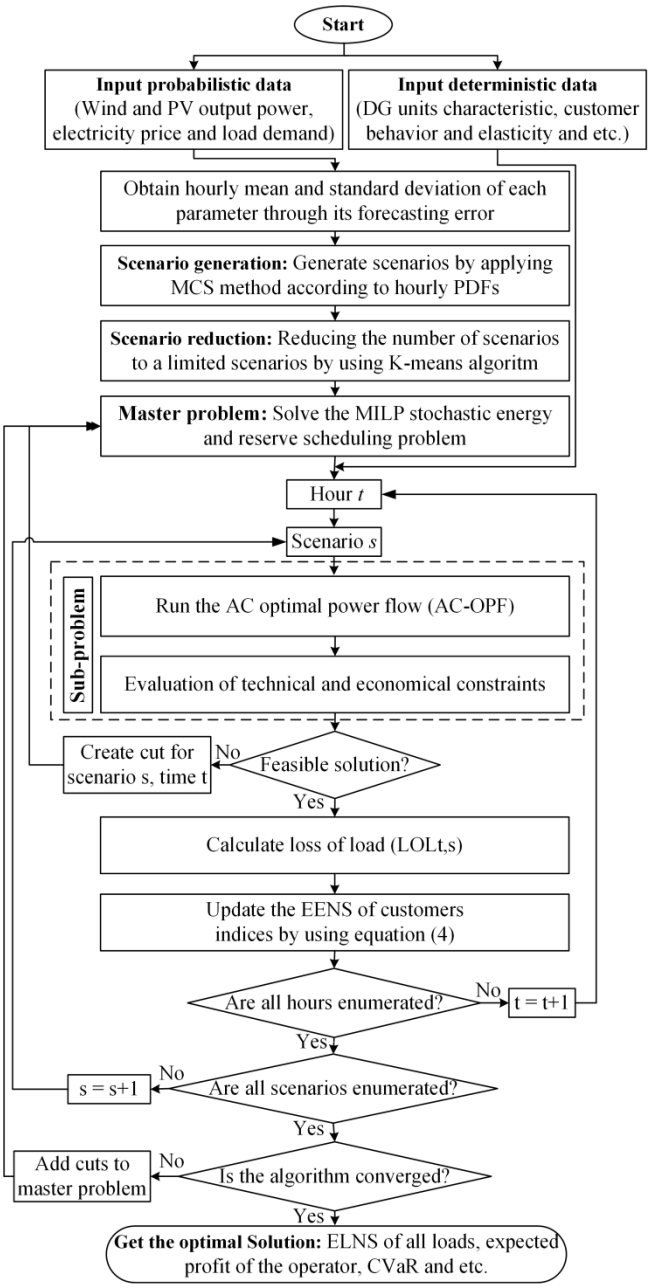

Fig. 1. Flowchart of the proposed computing procedure.

The solution from the master problem can be used as a running status for unit commitment problem. The vector of active power and outputs of committed DG units ($u_{i,t}$ and $p_{i,t}$

) obtained from the master problem are checked in the sub-problem stage from feasibility viewpoint. In the sub-problem stage, network security and system reliability constrains are considered and feasibility and optimality cuts are created in this optimization level. Network security constraints are checked by running AC-OPF and reliability is considered by LOL index. If network violation arises in any of the sub-problem, the benders cuts will be formed and added to the master problem for solving the next iteration of the optimization problem. The coupling between the master and the sub-problem is done through the variable $p_{i,t}^{*}$, which is the solution of problem represented by equations (1)-(56). The iterative process continues until the violations are eliminated and a solution is found.

The sub-problem can be formulated as:

$$Min \quad W = \sum^{N} \cos t_s slack \tag{66}$$

$$S \times LF - slack \le \sum_{i}^{N_G} p_i^{*} + \sum_{w}^{N_W} p_w^{*} + \sum_{v}^{N_V} p_v^{*} - \sum_{j=1}^{N_J} D_j \pi_{d1} \tag{67}$$

$$-S \times LF - slack \le -\sum_{i}^{N_G} p_i^{*} - \sum_{w}^{N_W} p_w^{*} - \sum_{v}^{N_V} p_v^{*} + \sum_{j=1}^{N_J} D_j \pi_{d2} \tag{68}$$

$$LF - \gamma S' = 0 \tag{69}$$

$$LF \le \overline{P_F} \pi_{LF1} \tag{70}$$

$$0 \le slack \le D_t \pi_{ds} \tag{71}$$

In the above equations, *slack* represents relaxation variable, $\cos t_s$ is infeasibility cost vector and usually set to one, and $p_{i,t}^{*}$ is unit commitment generation level vector. It should be noted that in the proposed solving methodology a set of inexpensive cuts to be added in the initial master problem, in order to provide early signals of the network to the unit commitment calculation.

The levels, master and sub-problems, are coupled by Benders cuts which are updated at each iteration for all operation problems. After solving the problem represented by equations (66)-(71), Benders feasibility cuts is generated based on sub-problem results for each hour of a network scenario as follows:

$$W^{*} + (\pi_{d1} - \pi_{d2})(p_{i,t} - p_{i,t}^{*}) \le 0 \tag{72}$$

Feasibility cuts are added to the master problem to enforce the feasibility of the slave problems. After solving the problem represented by (66)-(71), if all slack variables are zero, a feasible power flow is found. If certain slack variables are nonzero, their values are considered as a metric of the infeasibility and used to formulate feedback constraints to eliminate this infeasibility. Therefore, if AC-OPF analysis does not result in a feasible solution, an infeasibility cut is appended to the master problem and network constraints are fed back to the master problem for a revised solution to determine the schedule of DG units as well as load curtailments. This process will be repeated until a feasible solution is achieved for all scenarios. However, if the solution method could not converge to a feasible point in the sub-problem, an optimal cut is generated to be included in the master problem. At optimum point, the LOL and ELNS are calculated as the reliability indices, which are appropriate for assessing the variation of the reliability level in different hours of the next day. Moreover, the other decision variables of the optimization problem are power generations in scenario ($P_{i,t,s}$), deployed reserves of DG units ($r_{i,t,s}^{up}, r_{i,t,s}^{dn}$), and demand-side ($r_{j,t,s}^{up}, r_{j,t,s}^{dn}$), load demand after implementing DR programs ($D_{j,t,s}$), curtailed $LOL_{j,t,s}$, and $EENS_j$ for scenario and 24-hours. Therefore, the outcomes of the optimization problem provide the microgrid operator with the optimal scheduling of DG units, supply and demand-side reserves and a comprehensive insight into the reliability and economic aspects of the microgrid.

IV. Simulation and Numerical Results

A. Case Study and Main Assumptions

The proposed model is applied to a low-voltage autonomous microgrid detailed in [18]. The microgrid is composed of 16 nodes, five dispatchable DG units and three similar wind turbines (WTs) as well as two similar PV units. The technical and economic information of different DGs and RESs units is specified in Table II, [17], [18]. The microgrid supplies eight groups of aggregated loads that are equipped with smart power controllers to enable automated connectivity to end-use customers' control systems. The hourly load demand and the electricity prices along with the entire day

TABLE II
INFORMATION OF GENERATING UNITS

Unit	Min-Max generation capacity (kW)	Marginal cost ($/kWh)	Start-up cost ($)	Shut-down cost ($)	Cost of up-SR* ($)	Cost of down-SR ($)	Cost of non-SR ($)
DG_1	25-150	0.055	0.090	0.080	0.031	0.030	0.030
DG_2	25-150	0.068	0.090	0.080	0.031	0.030	0.030
DG_3	20-100	0.120	0.160	0.090	0.038	0.035	0.035
DG_4	20-100	0.142	0.160	0.090	0.038	0.035	0.035
DG_5	35-150	0.084	0.120	0.080	0.039	0.037	0.035
WT	0-80	0.055	-	-	-	-	-
PV	0-75	0.040	-	-	-	-	-

*SR: spinning reserve

This article has been accepted for publication in a future issue of this journal, but has not been fully edited. Content may change prior to final publication. Citation information: DOI 10.1109/TIA.2019.2959549, IEEE Transactions on Industry Applications

output power of wind and PV plants in different scenarios are presented in Fig. 2, [17]. In this figure, the red lines denote the mean of each parameter that are equal with their forecasted values and are extracted from [15], [18]. Moreover, it is assumed that prediction errors of the load, electricity price, wind and PV output powers follow the normal distributions with standard deviations equal to 20%, 15%, 10% and 10%, respectively, [18], [33]. The MCS method is used to generate 2000 initial scenarios with even probabilities and K-means algorithm is also implemented to the model to select 25 scenarios that represent well enough the uncertainties. All the results for the illustrative risk-constrained stochastic optimization model for the mentioned case study are obtained using CPLEX under GAMS software [34] on a PC with 4 GB of RAM and Intel Core i7@ 2.60 GHz processor.

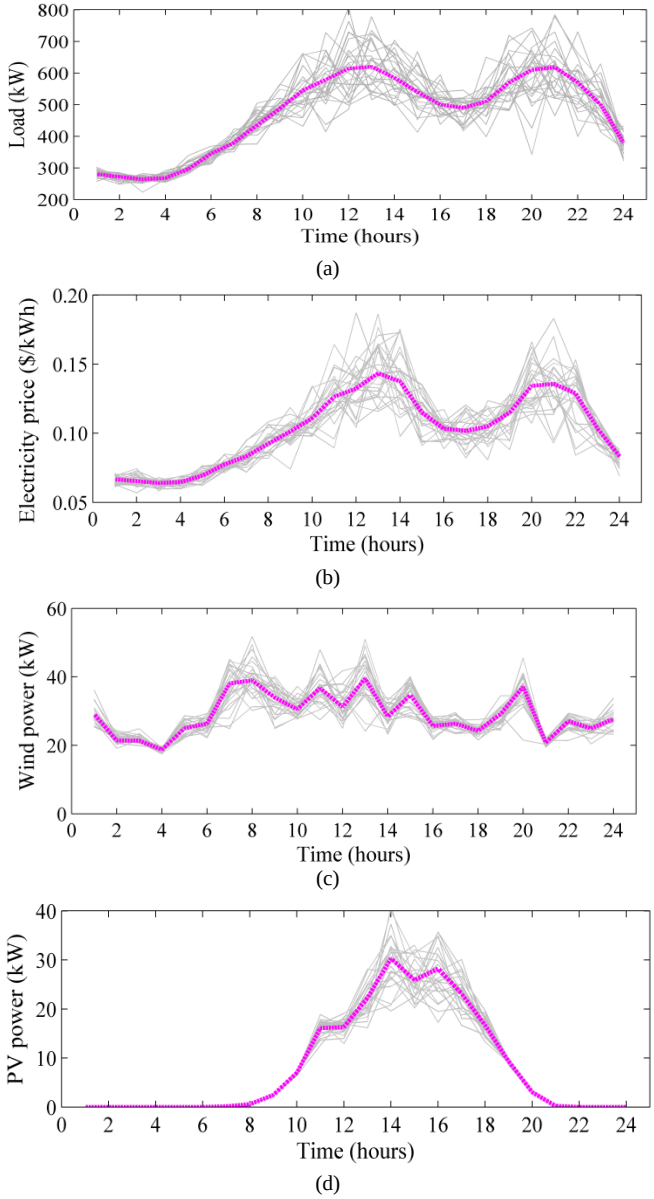

Fig. 2. Scenarios (grey lines) and the mean (red lines) related to each parameter [17], (a) Scenarios of demand load, (b) Scenarios associated with electricity price, (c) Scenarios of wind power, (d) Scenarios of PV power.

A 24-h horizon is chosen for the scheduling problem and the optimization problem is solved considering different values of the DR participants, risk aversion and reliability indices. Also, the optimality gap of different cases of the optimization algorithm is set to 0.0, and computation times for the proposed method under different operating conditions are less than 118 seconds (~2 min) in all cases with 39356 iterations in total.

B. Numerical Results

In this study, the results are analyzed in different levels of DR participation in both risk-neutral case (i.e., β=0) and risk-averse case (i.e., β=20). The effect of VOLL in different condition is investigated on the economic parameters. In all instances, the confidence level to compute CVaR is assumed to be 95%. Fig. 3 (a) and (b) depicts the operator's profit versus different DR participation rates and VOLLs for both risk-neutral and risk-averse cases, respectively. As shown, by increasing DR actions the expected profit increases in two cases.

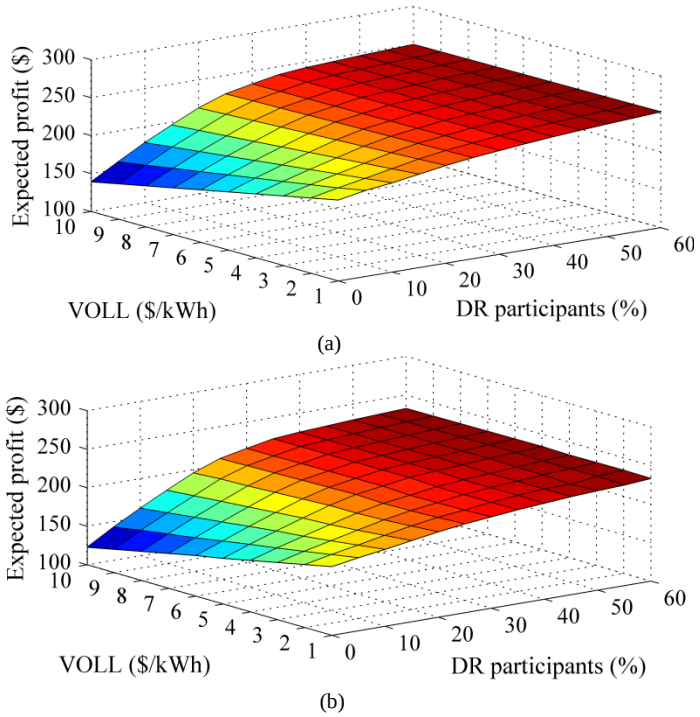

Fig. 3. Expected profit of operator versus VOLL and DR participants risk-neutral case (β=0), (b) risk-averse case (β=20).

When the customers' participation in DR programs increases, they reduce their power demands during peak hours by shedding some of their responsive loads and/or shifting a part of their consumption to low load periods. It causes the total generation costs decrease by dispatching less expensive DG units and as the result, the expected profit increases. Moreover, by increasing VOLL, in the lower levels of DR rates (i.e. less than 30%), although the amount of ENS reduces (due to allocating more reserve by DGs and DR), the product of VOLL and expected ENS (i.e. $Cost_{ENS}$) increases, and so, the expected profit decreases. In other word, in lower levels of DR participants and higher VOLLs, additional spinning reserve is much more cost-effective than the LOL imposed on

consumers. Therefore, in higher values of VOLLs, the costly generating units will be dispatched most of the times to reduce the ENS and consequently, the expected profit reduces especially when the rate of DR actions is low. However, by increasing the number of DR participants, the system uncertainties augment which in turn require more reserve allocation in higher VOLLs that leads to more ENS reduction. Therefore, as DR penetration rate increases, the decreasing ENS cost (i.e. $Cost_{ENS}$) compensates the increasing cost of reserve allocation (i.e. $Cost_R$), and as the result, the expected profit remains approximately constant. Furthermore, comparison of results in Fig. 4 shows that the profit in the risk-averse case is lower than that of in the risk-neutral case. This happens due to the fact that by increasing the weighting factor β, the operator is more risk-averse and buys more reserve capacity to accommodate the uncertainties and to mitigate the load shedding events.

The values of CVaR term versus DR penetration rate and VOLL for risk-neutral and risk-averse cases are shown in Fig. 4 (a) and (b), respectively. The CVaR is negative in two cases indicating that the profit in some scenarios is negative, i.e., there is a significant probability of experiencing losses.

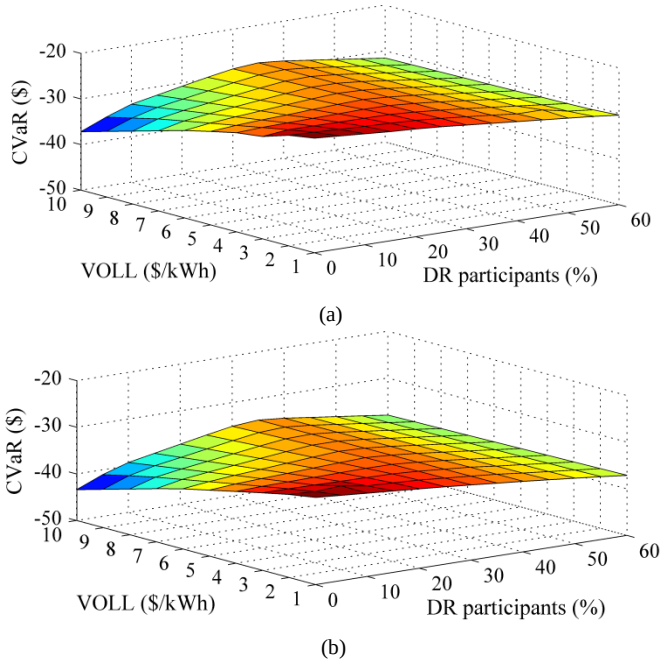

Fig. 4. CVaR versus VOLL and DR participants (a) risk-neutral case (β=0), (b) risk-averse case (β=20).

As observed, by increasing the number of DR participants, the CVaR increases initially but then decreases. This trend shows that the scenarios that provide the lowest profit in the profit maximization problem depend on the number of DR participants, meaning that in the lower levels of DR actions, the reserve allocated by responsive loads is used to hedge against wind and price volatility. However, when the number of DR participant increases up to a certain level, the volatility of responsive loads also increases due to their high dependency on volatility of the electricity prices and CVaR decreases accordingly. Moreover, as observed from Fig. 4, when VOLL increases, the CVaR decreases, especially in the lower levels of the DR actions. In fact, with higher VOLLs, the amount of total reserve capacity augments to mitigate the ENS in unwanted scenarios. However, by increasing the reserve allocation in higher DR rates, the amount of load shedding in undesired scenarios is reduced and as the result, the rising rate of CVaR diminishes. In addition, with higher values of risk factor, the effect of undesired scenarios increases and therefore the CVaR in the risk-averse case is higher than that of in the risk-neutral case.

Fig. 5 depicts the costs of generating units and payments of customers in different levels of DR participation for both risk-neutral and risk-averse cases. The cost of DG units is defined as the sum of their start-up, shut-down and operation costs. As shown, with increasing participation of customers in DR programs, the cost of energy supplied by dispatchable DGs is substantially reduced in both cases because of less operation of expensive DG units. However, risk-averse behavior of the operator has a minor effect on the operational costs of dispatchable DG units. Also, as can be seen from Fig. 5 (b), by increasing DR participation value, the reductions in customers' payments in both cases remain the same trends.

Fig. 6 (a)-(c) illustrates the costs of scheduled reserves of DGs, DR and cost of total reserves in different rates of DR action, VOLL and parameter β, respectively. As shown in Fig. 6 (a), by increasing DR actions, because of higher participation of responsive loads in reserve services, the reserve capacity allocation by DG units decreases. In fact, with more participation of customers in DR programs a more reserves capacity is required in order to accommodate their unpredictable variability and, thus, to maintain microgrid security and reliability.

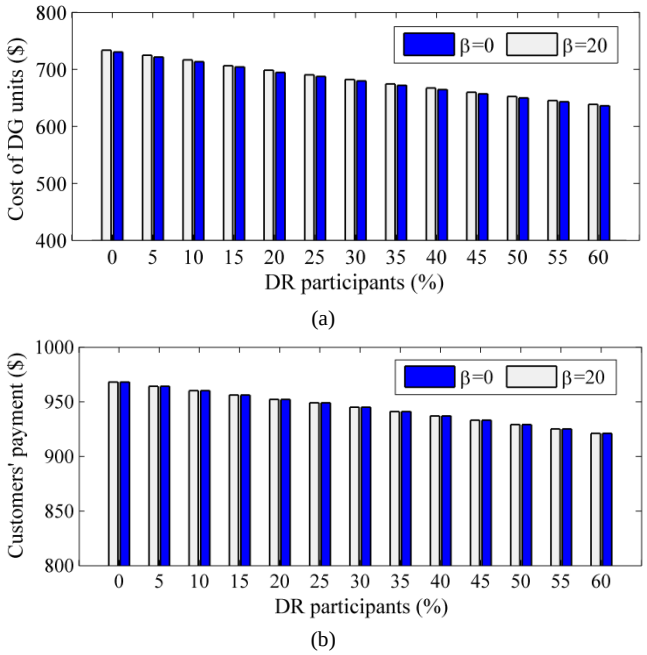

Fig. 5. (a) Operational costs of generating units, (b) payments of customers versus DR participants in two different values of parameter β.

Moreover, Fig. 6 (b) that illustrates cost of reserves under different VOLL in 30% DR participants shows that the costs of reserves increase by increasing VOLL values. Since, in higher values of VOLL, additional reserve is much more cost-effective than the load shedding imposed on consumers. In

fact, with increment of scheduled reserve in higher VOLL, the operator intends to eliminate costly load shedding events. Also, a similar trend is observed in Fig. 6 (c) that shows costs of reserves versus parameter β. As can be seen, by increasing values of β, the scheduled reserve increases to decrease the load shedding in undesired scenarios. When the operator becomes more risk-averse, it should allocate more reserves to avoid non-desirable profit distributions due to various worst scenarios.

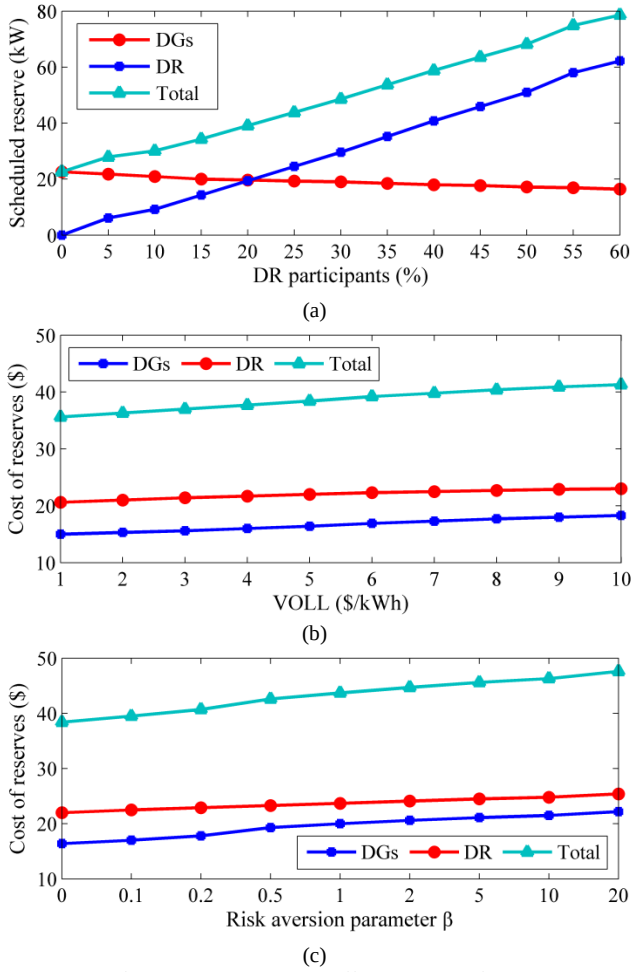

Fig. 6. Costs of scheduled reserves in different values of (a) DR participants, (b) VOLL, (c) risk aversion parameter β.

Fig. 7 shows the ELNS and its associated cost versus DR penetration rate in different values of VOLL. It can be seen that by increasing DR participants to 30%, the amount of EENS also reduces in all cases due to the reduction of LOL. Moreover, with more active contribution of end-use consumers in DR programs and allocating more reserve capacity through incorporating responsive loads, the amount of ENS decreases which ultimately ends in lower EENS cost. However, beyond a certain DR participation rate (here around 30% as can be understood from the figure), the EENS and its related cost remain almost unchanged as enough reserve capacity is allocated in the system and the ENS is reduced dramatically. Moreover, it is observed from Fig. 7 (b) that in higher VOLLs (i.e. VOLL =10 $/kWh) although the EENS is very small, the product of VOLL and expected ENS is relatively considerable. Therefore, to prevent excess payment to customer as EENS cost, the operator tries to provide more reserve in higher values of VOLL (see Fig. 6 (b)). It should be noted that, in the reliability-constrained scheduling problem, the operator tries to reduce the cost of security, which includes the cost of reserve capacity as well as the cost of EENS. Therefore, it should make a tradeoff between these two cost components to achieve higher system reliability.

To get more insight into the reliability aspects, total amount of LOL in scheduling horizon together with the cost of EENS in different VOLLs are illustrated in Table III. As it can be observed, the amount of LOL is decreased by increasing VOLL with and without considering DR actions. Moreover, computation times taken by the proposed scheduling approach are less than 8 minutes that is acceptable for day-ahead scheduling purposes It is further understood from the results that as the VOLL increases up to 8 $/kWh, more reserve is allocated by resources (see Fig. 7 (b)), thus no LOL occurs during the entire scheduling horizon with DR support. Therefore, by increasing VOLL and allocating more reserve by the microgrid resources, it is possible to form a reliable system and meet the system security constraints. Additionally, by increasing VOLL, the cost of EENS reduces with a higher rate when customers participate in DR program. In order to more investigate of the proposed model, it is illustrated using an illustrative example based on an IEEE 118-bus test system, as a practical larger-scale test system. Data for this system can be found in [35], [36]. Results of solving scheduling problem for this case study are provided in Table IV, which compared the total operating cost, expected profit, LOL and EENS for three values of VOLL in cases of with and without DR actions. The results confirm that larger VOLL enforces smaller total expected profit but also smaller LOL index. In fact, by increasing VOLL, the DGs operating costs increase that is mainly due to the fact that the more expensive units should be committed to satisfy the demand such that the LOL value decreases.

TABLE IV
THE RESULT OF THE PROPOSED SCHEDULING PROBLEM IN IEEE 118-BUS SYSTEM

VOLL ($/kWh)	DR participants (%)	Total operating cost ($)	Total expected profit ($)	Total LOL in scheduling horizon (MW)	Total cost of EENS in scheduling horizon ($)	Computation time (sec)
1	No DR	1656812	135132	62.3	62300	437
	With 60%	1634217	206112	5.2	5200	460
5	No DR	1659300	127254	35.8	179000	462
	With 60%	1642968	204501	2.3	11500	471
10	No DR	1664752	122200	12.0	120000	467
	With 60%	1651753	203723	0.2	2000	476

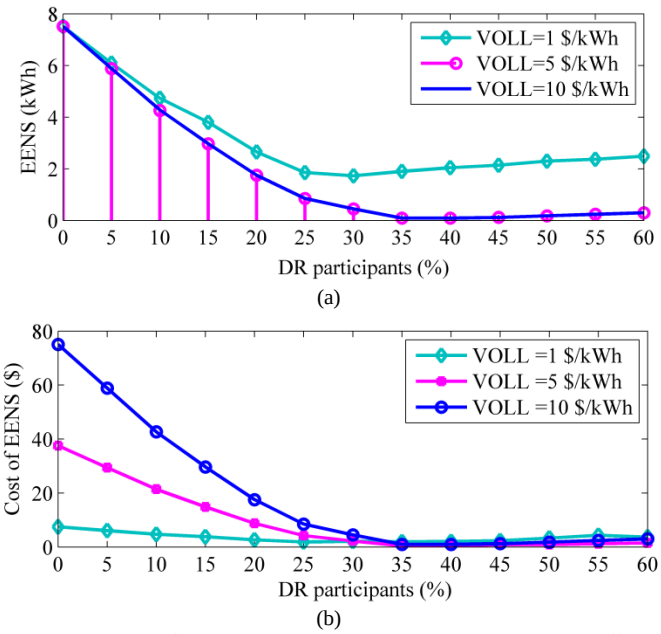

Fig. 7. The values of EENS and its costs versus DR participants in different values of VOLL, (a) EENS, (b) cost of EENS.

TABLE III
THE AMOUNT OF LOL AND COST OF EENS VERSUS VOLL

VOLL ($/kWh)	Total LOL in scheduling horizon (kW)		Total cost of EENS in scheduling horizon ($)	
	No DR	With DR	No DR	With DR
1	75.36	2.24	75.36	2.24
2	57.05	0.60	114.10	1.20
3	49.09	0.42	147.27	1.27
4	43.45	0.35	173.32	1.39
5	38.00	0.29	190.00	1.45
6	32.34	0.23	194.04	1.40
7	26.08	0.12	182.56	0.82
8	22.41	0	179.28	0
9	16.41	0	147.69	0
10	9.41	0	94.10	0

V. CONCLUSIONS

This paper studied the impacts of price-based DR programs and risk-aversion parameter on reliability and economy aspects of an autonomous microgrid. A risk-constrained stochastic model was developed to maximize the expected profit of the microgrid operator under uncertain behavior of wind and PV output power, day-ahead prices and demand. Furthermore, CVaR was used as a risk management function to enable operator to make a desirable trade-off between expected profit and risk levels. The performance of the proposed stochastic risk-constrained model was validated through simulating an autonomous microgrid with different dispatchable DGs, RESs and responsive loads. Moreover, various sensitivity analyses were performed to measure the impacts of DR participants and VOLL on the microgrid reliability and economy indices.

The summary of the numerical results obtained in the case study are as the below:

- By increasing VOLL, in lower levels of DR participants (i.e. less than 30%), the cost of ENS increases, and as the result, the expected profit of operator decreases. However, by increasing DR actions, the amount of reserve capacity allocated by responsive loads increases that leads to the ENS reduction.
- By increasing the number of DR participants, the CVaR increases initially but then decreases. In lower DR participation levels (i.e. less than 30%), the reserve allocated by responsive loads is used to hedge against wind and price volatility. However, when DR participation rate increases up to 30%, the volatility of responsive loads also increases due to their dependencies on volatility of the electricity prices which ultimately decreases the CVaR.
- When DR participation rate increases, the amount of EENS decreases at first. However, with more active participation of customers in DR programs and allocating more reserve by them, the EENS remain approximately unchanged.

As the future work, the proposed economic-reliability scheduling framework will be extended to optimal scheduling of multi-microgrid clusters in a distribution network where optimal decision-making of distribution system operator and multi-microgrids with inherently conflicting objectives must be addressed.

References

[1] H. Farzin, M. Fotuhi-Firuzabad, and M., Moeini- Aghtaie, "Stochastic Energy Management of Microgrids During Unscheduled Islanding Period," *IEEE Trans. on Ind. Info.*, Vol. 13, no. 3, pp. 1079-1087, 2017.

[2] A. Gholami, T. Shekari, F. Aminifar, and M. Shahidehpour, "Microgrid scheduling with uncertainty: the quest for resilience," *IEEE Trans. Smart Grid*, Vol. 30, no. 3, pp. 1337–1350, 2016.

[3] X. Xu, T. Wang, L. Mu, and J. Mitra, "Predictive Analysis of Microgrid Reliability Using a Probabilistic Model of Protection System Operation," *IEEE Trans. Power Syst.*, Vol. 32, no. 4, pp.3176-3184, 2017.

[4] V. Sarfi, and H. Livani, "An Economic-Reliability Security-Constrained Optimal Dispatch for Microgrids," *IEEE Trans. Power Syst.*, Vol. 33 , no. 6, pp. 6777-6786, 2018.

[5] M. Vahedipour-Dahraie, H. R. Najafi, A. Anvari-Moghaddam, and J. M. Guerrero, "Study the Effect of Time-Based Rate Demand Response Programs on Stochastic Day-Ahead Energy and Reserve Scheduling in Islanded Residential Microgrids," *Appl. Sci.* Vol. 7, no. 4, 378, pp. 1-19, 2017.

[6] M. L. Little, S. F. Rabbi, K. Pope, and, J. E. , "Quaicoe Unified Probabilistic Modeling of Wind Reserves for Demand Response and Frequency Regulation in Islanded Microgrids," *IEEE Trans. Industry Applications*, Vol. 54, no. 6, pp. 5671 – 5681, 2018.

[7] N. Mahmoudi, T. K. Saha, and M. Eghbal, "Demand Response Application by Strategic Wind Power Producers," *IEEE Trans. on Power syst.*, Vol. 31, no. 2, pp. 1227-1237, 2017.

[8] A. Dadkhah, B.Vahidi, "On the network economic, technical and reliability characteristics improvement through demand-response implementation considering consumers' behaviour," *IET Gen., Trans. & Dist.*, Vol. 12, no. 2, pp. 431-440, 2018.

[9] A. Moshari, A. Ebrahimi, and M. Fotuhi-firuzabad, "Short-term impacts of DR programs on reliability of wind integrated power systems considering demand-side uncertainties," *IEEE Trans. Power Syst.*, Vol. 31, no. 3, pp. 2481-2490, 2016.

[10] M. Rastegar, "Impacts of Residential Energy Management on Reliability of Distribution Systems Considering Customer Satisfaction Model," *IEEE Trans. Power Syst.*, Vol. 33 , no. 6, pp. 6062-6073, 2018.

[11] K. Kopsidays, and M. Abogaleela, "Utilizing Demand Response to Improve Network Reliability and Ageing Resilience," *IEEE Trans. Power Syst.*, Vol. 34, no. 3, pp. 2216–2227, 2019.

[12] E. Mahboubi-Moghaddam, M. Nayeripour, and J. Aghaei, "Reliability constrained decision model for energy service provider incorporating

demand response programs," *Applied Energy*, Vol. 183, pp. 552–565, 2016.

[13] G. Li, Y. Huang, and Z. Bie, "Reliability Evaluation of Smart Distribution Systems Considering Load Rebound Characteristics," *IEEE Trans. Sust. Energy*, Vol. 9, no. 4, pp. 1713-1721, 2018.

[14] M. Tavakoli, F. Shokridehaki, M.F. Akorede, M. Marzband , I. Vechiu, and E. Pouresmaeil, "CVaR-based energy management scheme for optimal resilience and operational cost in commercial building microgrids," *Int. J. of Elect. Power & Energy Syst.*, Vol. 100, pp. 1-9, 2018.

[15] D. T. Nguyen, and L. B. Le, "Risk-Constrained Profit Maximization for Microgrid Aggregators with Demand Response," *IEEE Trans. Smart Grid*, Vol. 6, no.1, pp. 135-146, 2015.

[16] M. Vahedipour-Dahraie, H. Rashidizaheh-Kermani, H. R. Najafi, A. Anvari-Moghaddam, and J. M. Guerrero, "Stochastic Security and Risk-Constrained Scheduling for an Autonomous Microgrid with Demand Response and Renewable Energy Resources," *IET Renewable Power Generation*, Vol. 11, no. 14, pp. 1812-1821, 2017.

[17] M. Vahedipour-Dahraie, A. Anvari-Moghaddam, and J. M. Guerrero, "Evaluation of Reliability in Risk-Constrained Scheduling of Autonomous Microgrids with Demand Response and Renewable Resources," *IET Renewable Power Generation*, Vol. 12, no. 6, pp. 657 – 667, 2018.

[18] M. Vahedipour-Dahraie, H. Rashidizaheh-Kermani, H. R. Najafi, A. Anvari-Moghaddam, and J. M. Guerrero, "Stochastic Frequency-Security Constrained Scheduling of a Microgrid Considering Price-Driven Demand Response," International Symposium on Power Electronics, Electrical Drives, Automation and Motion (SPEEDAM), 20-22 June 2018, Amalfi, Italy, pp. 716-721, 2018.

[19] Y. Liu, Y. Li, H. B. Gooi, Y. Jian, H. Xin, X. Jiang, and J. Pan, "Distributed Robust Energy Management of a Multimicrogrid System in the Real-Time EnergyMarket*," IEEE Trans. Sust. Energy*, Vol. 10, no. 1, pp. 396-406, 2019.

[20] H. Mohsenian-Rad, "Optimal Demand Bidding for Time-Shiftable Loads," *IEEE Trans. Power Syst*., Vol. 30, no. 2, pp. 939-951, 2015.

[21] G. Graditi, M. L. D. Silvestre, R. Gallea, and E. R. Sanseverino "Heuristic-based shiftable loads optimal management in smart micro-grids," *IEEE Trans. on Industrial Informatics*, Vol. 11, no. 1, pp. 271-280, 2015.

[22] M. Nikzad and B. Mozafari, "Reliability assessment of incentive- and priced-based demand response programs in restructured power systems," *Elect. Power Energy Syst.*, vol. 56, pp. 83–96, Mar. 2014.

[23] A. Abdollahi, M. Parsa Moghaddam, M. Rashidinejad, and M.K. Sheikh-El-Eslami, "Investigation of Economic and Environmental-Driven Demand Response Measures Incorporating UC," *IEEE Trans. Smart Grid*, vol. 3, no.1, pp. 12-25, 2012.

[24] Y. Guo, S. Li, C. Li, and H. Peng, "Short-Term Reliability Assessment for Islanded Microgrid Based on Time-Varying Probability Ordered Tree Screening Algorithm*," IEEE Access*, Vol. 7, pp. 37324-37333, 2019.

[25] D. Gan, D. Feng, and J. Xie, "Electricity Markets and Power System Economics*,"* CRC Press, 1st Edition, 2013.

[26] C. Joe-Won, S. Sen, S. Ha, and M. Chiang, "Optimized day-ahead pricing for smart grids with device-specific scheduling flexibility," *IEEE J. Sel. Areas Commun.*, Vol. 30, no. 6, pp. 1075-1085, 2012.

[27] P.A. Trodden, W.A. Bukhsh A. Grothey and K.I. McKinnon, "Optimization-based islanding of power networks using piecewise linear ac power flow," *IEEE Trans. Power Syst.* Vol. 29, no. 3, pp. 1212-1220, 2014.

[28] M. Carrión, J. M. Arroyo, and A. J. Conejo, "A Bilevel Stochastic Programming Approach for Retailer Futures Market Trading," *IEEE Trans. on power systems*, vol. 24, no. 3, 2009.

[29] L. Wu, M. Shahidehpour, and T. Li, "Cost of reliability analysis based stochastic unit commitment," *IEEE Trans. Power Syst.*, Vol. 23, no. 3, pp. 1364–1374, 2008.

[30] R.M. Korwar, "On stochastic orders for sums of independent random variables," *J. Multivar. Anal.*, Vol. 80, pp. 344–357, 2002.

[31] J. Toubeau, J. Bottieau, F. Vallée, and Z. D. Grève, "Deep Learning-Based Multivariate Probabilistic Forecasting for Short-Term Scheduling in Power Markets*," IEEE Trans. Power Syst.*, Vol. 34, no. 2, 1203-1215, 2019.

[32] D. Arthur, and S. Vassilvitskii, "K-means++: The advantages of careful seeding," in Proc. 18th Annu. ACM-SIAM Symp Discrete Algorithms (SODA '07), New Orleans, LA, USA, pp. 1027-1035, 2007.

[33] N. Rezaei, and M. Kalantar, "Smart microgrid hierarchical frequency control ancillary service provision based on virtual inertia concept: An integrated demand response and droop controlled distributed generation framework," *Energy Conversion and Management*, Vol. 92, pp. 287-301, 2015.

[34] "The General Algebraic Modeling System (GAMS) Software," online available at: http://www.gams.com, accessed on 15 September 2016.

[35] H. Yamin, A. Kamel, and M. Shahidehpour, "New approach for dynamic optimal power flow using benders decomposition in a deregulated power market," *Elect Power Syst Res.*, Vol. 62, no. 2, pp. 101-107, 2003.

[36] J.K. Lyu, M.K. Kim, Y.T. Yoon, and J.K. Park, "A new approach to security-constrained generation scheduling of large-scale power systems with a piecewise linear ramping model," *Electrical Power and Energy Systems*, Vol. 34, pp. 121–131, 2012.